Electromagnetically induced transparency based six-wave mixing in a Doppler-broadened folded four-level system*

Niu Jin-Yan(牛金艳), Pei Li-Ya(裴丽娅), Wu Ling-An(吴令安), and Fu Pan-Ming (傅盘铭)†

Laboratory of Optical Physics, Institute of Physics and Center for Condensed Matter, Chinese Academy of Sciences, Beijing 100190, *China*

(Received 8 March 2010; revised manuscript received 25 May 2010)

We study phase-conjugate six-wave mixing spectroscopy based on electromagnetically-induced-transparency in a Doppler-broadened folded four-level system. It is found that the six-wave mixing spectrum can be either Doppler-free or very broad, depending on whether the interference between the polarisations of atoms with different velocities is constructive or destructive. To obtain the Doppler-free six-wave mixing spectrum in the folded four-level system, the conditions are more stringent in comparison with those in the cascade and N-type four-level systems. This polarisation interference can be controlled in the presence of a strong coupling field.

Keywords: six-wave mixing, electromagnetically induced transparency, polarisation interference
PACC: 3290, 4265M

1. Introduction

Resonant enhanced wave-mixing processes have been a subject of intense research for many years. When the frequencies of the incident light beams passing through a nonlinear medium coincide with the atomic or molecular resonances, the signal will be enhanced tremendously, thus wave-mixing with resonant excitations can be employed as a versatile spectroscopic technique.[1] Up to now, most of these studies have been concerned with four-wave mixing (FWM). For example, several resonance-enhanced nondegenerate FWM schemes have been developed by our laboratory for various spectroscopic purposes.[2−6] Moreover, if an additional strong coupling field is applied, then the FWM spectrum exhibits Autler–Townes (AT) splitting, which provides a new spectroscopic tool for measuring not only the resonant frequency and dephasing rate but also the transition dipole moment between two highly excited atomic states.[7,8]

Recently, higher-order wave-mixing effects have attracted much attention.[9−17] Moore *et al.*[9] have observed axially propagating phase-matched FWM and six-wave mixing (SWM) in pure sodium vapour under near-resonant two-photon excitations. Kang *et al.*[10] have reported a type of resonant SWM in an N-type four-level system, where electromagnetically induced transparency (EIT) suppresses the linear susceptibility and enhances the nonlinear susceptibilities, leading to resonantly enhanced, slow-photon SWM at low light intensities. On the other hand, we proposed a generalised phase-conjugate $2n$-wave mixing scheme, where a phase matching geometry allows us to isolate higher order wave mixing.[18] This method provides information about the relaxation of high-order atomic coherence and so is particularly suitable for studying highly excited atomic states or states with high angular momentum.

One phenomenon which attracts relatively little attention is that in a Doppler-broadened system there exists interference between polarisations of atoms of different velocities.[19] This polarisation interference can cause significant modification of the SWM spectrum. For example, due to the polarisation interference the SWM spectrum in Doppler-broadened cascade or N-type four-level systems can be either Doppler-free or very broad, depending on the directions of the incident beams and the ratios between the magnitudes of the wave vectors.[20,21] In this paper, we shall study SWM in a Doppler-broadened folded four-level system. It is found that the polarisation interference is extremely sensitive to the energy level structure. To obtain Doppler-free SWM spectrum in

*Project supported by the National Natural Science Foundation of China (Grant Nos. 10774185, 10974252, and 10674174), and the National Program for Basic Research in China (Grant No. 2006CB921107).
†Corresponding author. E-mail: pmfu@aphy.iphy.ac.cn
© 2010 Chinese Physical Society and IOP Publishing Ltd

the folded four-level system the conditions are more stringent in comparison with those in the cascade and N-type four-level systems. We also study how to control the polarisation interference by quantum interference when a strong coupling field is present.

2. Basic theory

Let us consider a folded four-level system (Fig. 1), where the states between $|0\rangle$ and $|1\rangle$, $|1\rangle$ and $|2\rangle$, and $|2\rangle$ and $|3\rangle$ are coupled by dipolar transitions with resonant frequencies Ω_1, Ω_2 and Ω_3, and dipole moment matrix elements μ_1, μ_2, and μ_3, respectively. In SWM, beams 3 and $3'$ have the same frequency ω_3 with a small angle between them. Beam 1 of frequency ω_1 propagates along the opposite direction to beam 3, while beam 2 of frequency ω_2 can propagate either along or opposite to the direction of beam 3. Assume that $\omega_i \simeq \Omega_i$ ($i = 1, 2$ or 3), so that ω_i drives the transition from $|i-1\rangle$ to $|i\rangle$. The simultaneous interactions of the atoms with beams 1, 2 and $3'$ will induce atomic coherence between $|0\rangle$ and $|3\rangle$ through a resonant three-photon transition. This three-photon coherence is then probed by beams 3 and 2, and as a result an SWM signal of frequency ω_1 is generated almost opposite to the direction of beam $3'$.

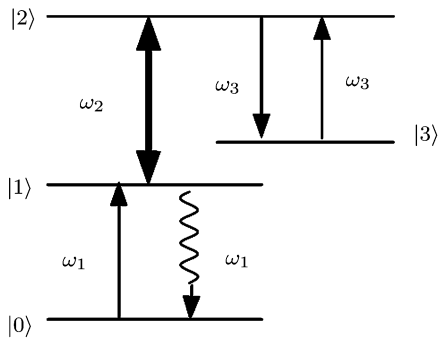


Fig. 1. Energy-level diagram for resonant SWM in a folded four-level system.

Let the detunings be represented by $\Delta_i = \Omega_i - \omega_i$, so after a canonical transformation the effective Hamiltonian is

$$\begin{aligned} H =& \hbar\Delta_1|1\rangle\langle 1| + \hbar(\Delta_1+\Delta_2)|2\rangle\langle 2| \\ &+ \hbar(\Delta_1+\Delta_2-\Delta_3)|3\rangle\langle 3| \\ &- [\mu_1 E_1|1\rangle\langle 0| + \mu_2 E_2|2\rangle\langle 1| \\ &+ \mu_3(E_3+E_3')|3\rangle\langle 2| + \text{H.c}], \end{aligned} \tag{1}$$

here, E_i and E_3' are the complex incident laser fields of beams i and $3'$, respectively. From perturbation theory the fifth-order off-diagonal density matrix element $\rho_{10}^{(5)}$, which is responsible for the SWM signal, is given by

$$\begin{aligned} \rho_{10}^{(5)} =& \frac{\mathrm{i}\,\mu_1\mu_2^2\mu_3^2}{\hbar^5}\int_0^\infty\int_0^\infty\cdots\int_0^\infty \mathrm{d}\tau_1\mathrm{d}\tau_2\cdots\mathrm{d}\tau_5 \\ &\times E_1(t-\tau_1-\tau_2-\tau_3-\tau_4-\tau_5) \\ &\times E_2(t-\tau_2-\tau_3-\tau_4-\tau_5) \\ &\times [E_3'(t-\tau_3-\tau_4-\tau_5)]^* \\ &\times E_3(t-\tau_4-\tau_5)E_2^*(t-\tau_5) \\ &\times \mathrm{e}^{-(\mathrm{i}\,\Delta_1+\Gamma_{10})(\tau_1+\tau_5)}\mathrm{e}^{-[\mathrm{i}(\Delta_1+\Delta_2)+\Gamma_{20}](\tau_2+\tau_4)} \\ &\times \mathrm{e}^{-[\mathrm{i}(\Delta_1+\Delta_2-\Delta_3)+\Gamma_{30}]\tau_3}, \end{aligned} \tag{2}$$

here, Γ_{i0} is the transverse relaxation rate between states $|i\rangle$ and $|0\rangle$, $E_i(t') = \varepsilon_i \mathrm{e}^{\mathrm{i}\,\boldsymbol{k}_i\cdot\boldsymbol{r}(t')}$ with $\mathbf{r}(t') = \boldsymbol{r}(t) - (t-t')\boldsymbol{v}$. Integrating over the τ_i's, we obtain

$$\begin{aligned} \rho_{10}^{(5)}(\boldsymbol{r},\boldsymbol{v}) =& \frac{\mathrm{i}\,S(\boldsymbol{r})}{(\mathrm{i}\,\Delta_1^d+\Gamma_{10})[\mathrm{i}(\Delta_1^d+\Delta_2^d)+\Gamma_{20}]} \\ &\times \frac{1}{[\mathrm{i}(\Delta_1^d+\Delta_2^d-\Delta_3'^d)+\Gamma_{30}]} \\ &\times \frac{1}{[\mathrm{i}(\Delta_1^d+\Delta_2^d-\Delta_3'^d+\Delta_3^d)+\Gamma_{20}]} \\ &\times \frac{1}{[\mathrm{i}(\Delta_1^d-\Delta_3'^d+\Delta_3^d)+\Gamma_{10}]}, \end{aligned} \tag{3}$$

where $\Delta_i^d = \Delta_i + \boldsymbol{k}_i\cdot\boldsymbol{v}$ and $\Delta_3'^d = \Delta_3 + \boldsymbol{k}_3'\cdot\boldsymbol{v}$ are the Doppler-shift frequency detunings, $S(\boldsymbol{r}) = G_1|G_2|^2G_3(G_3')^*\mathrm{e}^{\mathrm{i}(\boldsymbol{k}_1+\boldsymbol{k}_3-\boldsymbol{k}_3')\cdot\boldsymbol{r}}$, and the G's denote the coupling coefficients, i.e., $G_i = \mu_i\varepsilon_i/\hbar$ and $G_3' = \mu_3\varepsilon_3'/\hbar$. In a Doppler-broadened system the nonlinear polarisation $P^{\mathrm{NL}}(\boldsymbol{r})$ responsible for the SWM signal is given by averaging over the velocity distribution function $W(\boldsymbol{v})$, i.e.,

$$P^{\mathrm{NL}}(\boldsymbol{r}) = N\mu_1\textstyle\int_{-\infty}^{\infty}\mathrm{d}\boldsymbol{v}\ W(\boldsymbol{v})\rho_{10}^{(5)}(\boldsymbol{r},\boldsymbol{v}), \tag{4}$$

here, N is the density of the atoms, while $W(\boldsymbol{v}) = (1/\sqrt{\pi}u)\mathrm{e}^{-(v/u)^2}$, where $u = \sqrt{2kT/m}$ with m being the mass of an atom, k is Boltzmann's constant, and T the absolute temperature. The SWM signal intensity is proportional to $|P^{\mathrm{NL}}(\boldsymbol{r})|^2$.

Now, according to Eqs. (2) and (4), $P^{\mathrm{NL}}(\boldsymbol{r})$ can also be expressed as

$$\begin{aligned} P^{\mathrm{NL}}(\boldsymbol{r}) =& \mathrm{i}\,N\mu_1 S(\boldsymbol{r})\int_0^\infty\mathrm{d}\tau_1\cdots\int_0^\infty\mathrm{d}\tau_5 \\ &\times \mathrm{e}^{-(\mathrm{i}\,\Delta_1+\Gamma_{10})(\tau_1+\tau_5)}\mathrm{e}^{-[\mathrm{i}(\Delta_1+\Delta_2)+\Gamma_{20}](\tau_2+\tau_4)} \\ &\times \mathrm{e}^{-[\mathrm{i}(\Delta_1+\Delta_2-\Delta_3)+\Gamma_{30}]\tau_3}L(\tau_1,\tau_2,\tau_3,\tau_4,\tau_5), \end{aligned} \tag{5}$$

where $L(\tau_1,\tau_2,\tau_3,\tau_4,\tau_5)$ is defined as

$$L = \int_{-\infty}^{\infty}\mathrm{d}\boldsymbol{v}\ W(\boldsymbol{v})\mathrm{e}^{-\mathrm{i}\,\boldsymbol{k}_1\cdot\boldsymbol{v}\tau_1}\mathrm{e}^{-\mathrm{i}(\boldsymbol{k}_1+\boldsymbol{k}_2)\cdot\boldsymbol{v}\tau_2}$$

$$\times \mathrm{e}^{-\mathrm{i}(\boldsymbol{k}_1+\boldsymbol{k}_2-\boldsymbol{k}_3')\cdot\boldsymbol{v}\tau_3}\mathrm{e}^{-\mathrm{i}(\boldsymbol{k}_1+\boldsymbol{k}_2-\boldsymbol{k}_3'+\boldsymbol{k}_3)\cdot\boldsymbol{v}\tau_4}$$
$$\times \mathrm{e}^{-\mathrm{i}(\boldsymbol{k}_1-\boldsymbol{k}_3'+\boldsymbol{k}_3)\cdot\boldsymbol{v}\tau_5}. \quad (6)$$

We set $\boldsymbol{k}_1 = -k_1\boldsymbol{z}$ and $\boldsymbol{k}_3 = k_3\boldsymbol{z}$, while $\boldsymbol{k}_3'$ is approximated as $\boldsymbol{k}_3' \simeq k_3\boldsymbol{z}$ because the angle between beams 3 and 3′ is typically very small. On the other hand, since the phase matching condition is not dependent on the direction of beam 2, the latter can propagate either along the forward (i.e., $\boldsymbol{k}_2 = k_2\boldsymbol{z}$) or along the backward direction (i.e., $\boldsymbol{k}_2 = -k_2\boldsymbol{z}$). After integrating over the velocity, we have

$$L = \mathrm{e}^{-(k_1u/2)^2[(\tau_1+\tau_5)+(1-\zeta_2)(\tau_2+\tau_4)+(1-\zeta_2+\zeta_3)\tau_3]^2} \quad (7)$$

for the case of beam 2 propagating in the forward direction, while

$$L = \mathrm{e}^{-(k_1u/2)^2[(\tau_1+\tau_5)+(1+\zeta_2)(\tau_2+\tau_4)+(1+\zeta_2+\zeta_3)\tau_3]^2} \quad (8)$$

for the backward direction case. Here, $\zeta_2 = k_2/k_1$ and $\zeta_3 = k_3/k_1$ denote the ratios between the magnitudes of the wave vectors. We note that all values of τ_i (i = 1 to 5) are positive.

3. Polarisation interference in SWM

We present numerical results for the SWM spectra in a Doppler-broadened system with $\Gamma_{10}/k_1u = 0.02$, $\Gamma_{20}/\Gamma_{10} = \Gamma_{30}/\Gamma_{10} = 1$. We first consider the case in which beam 2 propagates along the forward direction. Figure 2 shows the SWM spectra when Δ_3 is scanned and $\Delta_1/\Gamma_{30} = \Delta_2/\Gamma_{30} = 0$, $\zeta_3 = 0.8$, for different values of the wave vector ratios: (a) $\zeta_2 = 0.5$ (solid curve), 0.7 (dashed curve), 0.9 (dotted curve) and (b) $\zeta_2 = 1.1$ (solid curve), 1.2 (dashed curve), 1.5 (dotted curve). At first, the SWM spectrum is very broad when $\zeta_2 < 1$ (Fig. 2(a)), where the linewidth decreases with the increase of ζ_2. The linewidth then decreases sharply and finally the spectrum becomes Doppler-free when $\zeta_2 > 1$ (Fig. 2(b)).

The SWM intensity as a function of Δ_1 or Δ_2 shows similar behaviour. For example, in Fig. 3 the SWM spectra is plotted against Δ_1 for $\Delta_2/\Gamma_{30} = \Delta_3/\Gamma_{30} = 0$, $\zeta_3 = 0.8$, and (a) $\zeta_2 = 0.5$ (solid curve), 0.7 (dashed curve), 0.9 (dotted curve); (b) $\zeta_2 = 1$ (solid curve), ≥ 1.1 (dashed curve). The drastic change of the linewidth at $\zeta_2 \simeq 1$ also appears in the ζ_2-dependence of the SWM signal intensity.

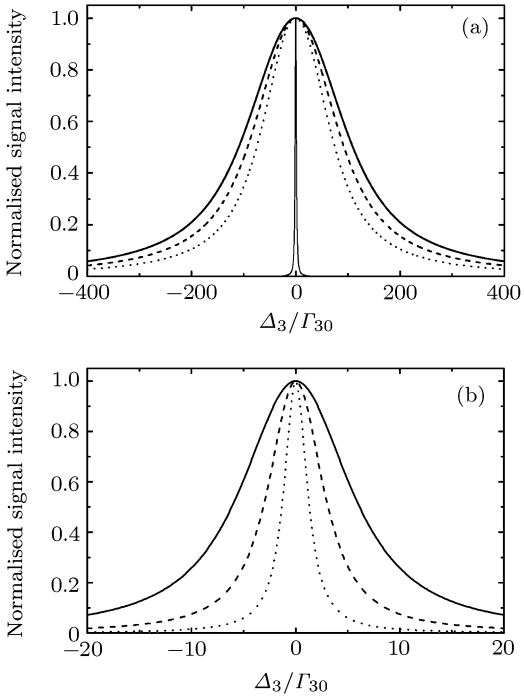


Fig. 2. SWM intensity versus Δ_3 when beam 2 propagates along the forward direction with parameters $\Delta_1/\Gamma_{30} = \Delta_2/\Gamma_{30} = 0$, and ζ_3 =0.8 for: (a) $\zeta_2 = 0.5$ (solid curve), 0.7 (dashed curve), 0.9 (dotted curve) and (b) $\zeta_2 = 1.1$ (solid curve), 1.2 (dashed curve), 1.5 (dotted curve). The thin solid curve in (a) represents the corresponding result when polarisation interference is neglected.

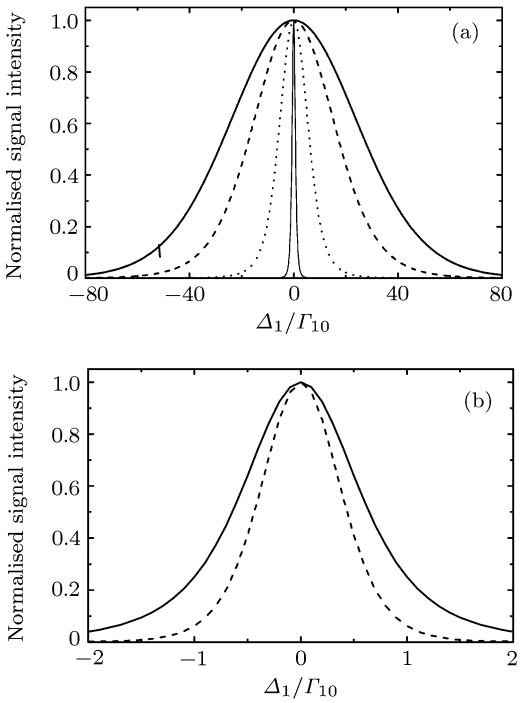


Fig. 3. SWM intensity versus Δ_1 when beam 2 propagates along the forward direction with parameters $\Delta_2/\Gamma_{30} = \Delta_3/\Gamma_{30} = 0$, and $\zeta_3 = 0.8$ for: (a) $\zeta_2 = 0.5$ (solid curve), 0.7 (dashed curve), 0.9 (dotted curve); (b) $\zeta_2 = 1$ (solid curve), ≥ 1.1 (dashed curve). The thin solid curve in (a) represents the corresponding result when polarisation interference is neglected.

Figure 4 presents the signal intensity as a function of ζ_2 with the following parameters: $\Delta_1/\Gamma_{30} = \Delta_2/\Gamma_{30} = \Delta_3/\Gamma_{30} = 0$ and $\zeta_3 = 0.8$. The SWM signal intensity increases by many orders of magnitude as the value of ζ_2 passes through 1. We next investigate the SWM spectrum when beam 2 propagates along the backward direction. It is found that for different values of ζ_s and ζ_3 the SWM spectra are always very broad. For example, Fig. 5 presents the SWM spectra against Δ_3 when $\Delta_1/\Gamma_{30} = \Delta_2/\Gamma_{30} = 0$, $\zeta_3 = 0.8$, and $\zeta_2 = 2$ (solid curve), 1.2 (dashed curve), 0.5 (dotted curve). Here, unlike the forward direction case (Fig. 2(a)), the linewidth increases as ζ_2 increases.

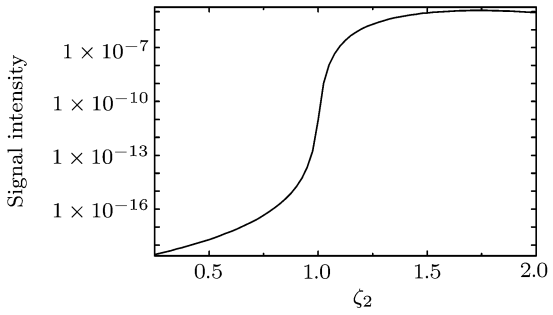


Fig. 4. SWM signal intensity as a function of ζ_2 when beam 2 propagates along the forward direction with $\Delta_1/\Gamma_{30} = \Delta_2/\Gamma_{30} = \Delta_3/\Gamma_{30} = 0$ and $\zeta_3 = 0.8$.

The broadband lineshapes of the SWM spectra shown in Figs. 2(a), 3(a) and 5 are in contradiction with the intuition that the spectra should be Doppler-free because only atoms in a specific velocity group will contribute to the signal. This anomalous behaviour of the SWM spectra is due to the destructive interference between the fields generated by the polarisations of atoms which have different velocities. For demonstration, instead of calculating $|\int_{-\infty}^{\infty} \mathrm{d}v\ \mathrm{e}^{-(v/u)^2}\rho_{10}(\boldsymbol{r},\boldsymbol{v})|^2$ we sum up the signal intensities of individual atoms, i.e., $\int_{-\infty}^{\infty} \mathrm{d}v\ \mathrm{e}^{-(v/u)^2}|\rho_{10}(\boldsymbol{r},\boldsymbol{v})|^2$ so the polarisation interference is neglected (thin solid curves in Figs. 2(a), 3(a) and 5). It is found that the lineshape is narrow and basically independent of the values of ζ_2 and ζ_3 when the polarisation interference is neglected. This indicates that the anomalous behaviour of the SWM spectra is due to the polarisation interference. Similar phenomena have been observed in the SWM spectra in cascade and N-type four-level systems.[18,19]

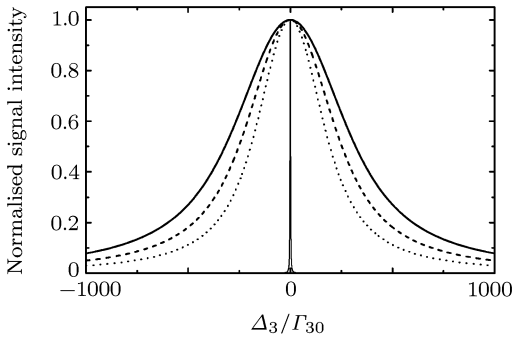


Fig. 5. SWM intensity versus Δ_3 when beam 2 propagates along the backward direction with $\Delta_1/\Gamma_{30} = \Delta_2/\Gamma_{30} = 0$, $\zeta_3 = 0.8$, and $\zeta_2 = 2$ (solid curve), 1.2 (dashed curve), 0.5 (dotted curve). The thin solid curve represents the corresponding result when polarisation interference is neglected.

Now, we analyse the polarisation interference in SWM based on the function $L(\tau_1, \tau_2, \tau_3, \tau_4, \tau_5)$. Physically, L involves integration over the velocity distribution function as shown in Eq. (6), therefore it reflects the degree of coherence between polarisations of atoms which have different velocities. The coherence between atomic polarisations is maximum when $L = 1$, leading to complete constructive interference. In this case, a Doppler-free SWM spectrum can be obtained. By contrast, $L \ll 1$ means that the phases of the polarisations of atoms with different velocities are basically random and we have very broad SWM spectra. Therefore, the characteristics of the SWM spectrum can be specified simply by examining the function $L(\tau_1, \tau_2, \tau_3, \tau_4, \tau_5)$. Let us first consider the case when beam 2 propagates along the forward direction. According to Eq. (7), the condition for $L = 1$ is

$$(\tau_1 + \tau_5) + (1 - \zeta_2)(\tau_2 + \tau_4) + (1 - \zeta_2 + \zeta_3)\tau_3 = 0. \quad (9)$$

Since all values of τ_i ($i = 1$ to 5) are positive, the above equation can be satisfied only if $\zeta_2 > 1$. This is consistent with the results shown in Figs. 2, 3 and 4. Now, we consider the case when beam 2 propagates along the backward direction. From Eq. (8), the condition for $L = 1$ is

$$(\tau_1 + \tau_5) + (1 + \zeta_2)(\tau_2 + \tau_4) + (1 + \zeta_2 + \zeta_3)\tau_3 = 0. \quad (10)$$

This can be satisfied only when $\tau_1 = \tau_2 = \tau_3 = \tau_4 = \tau_5 = 0$. Thus, we always have a very broad SWM spectrum (see Fig. 5) when beam 2 propagates along the backward direction.

Finally, based on the function L we can explain the ζ_2-dependence of the SWM linewidth when the spectrum is very broad. Let us first consider the case in which beam 2 propagates along the forward direction. According to Eq. (7), for the same values of τ's, L decreases with the decrease of ζ_2 when $\zeta_2 < 1$, indicating that the polarisation interference becomes more destructive. As a result, we have an increase of the SWM linewidth when ζ_2 is decreased (see Fig. 2(a)). By contrast, for the backward direction case, L decreases with the increase of ζ_2 according to Eq. (8), thus, the SWM becomes broader when ζ_2 increases (Fig. 5).

4. EIT-based SWM

Let us consider SWM based on EIT when beam 2 of frequency ω_2 is a strong field. We assume that ε_1, ε_3, and ε_3' are weak, whereas ε_2 can be of arbitrary magnitude, thus ρ_{10} needs to be calculated to the order $\varepsilon_1\varepsilon_3\varepsilon_3'$, but to all orders in ε_2. This can be done using density matrix equations with relaxation terms properly included

$$\frac{\mathrm{d}\rho}{\mathrm{d}t} = -\frac{\mathrm{i}}{\hbar}[H,\rho] + \left(\frac{\mathrm{d}\rho}{\mathrm{d}t}\right)_{\mathrm{relax}}. \tag{11}$$

Considering the Doppler shift of the frequency, we obtain

$$\rho_{10}^{(5)}(\boldsymbol{r},\boldsymbol{v}) = \frac{\mathrm{i}\,S(\boldsymbol{r})}{\{(\mathrm{i}\,\Delta_1^d + \Gamma_{10})[\mathrm{i}(\Delta_1^d + \Delta_2^d) + \Gamma_{20}] + |G_2|^2\}^2} \times \frac{1}{[\mathrm{i}(\Delta_1^d + \Delta_2^d - \Delta_3^d) + \Gamma_{30}]}. \tag{12}$$

Here, we assume that $\Delta_3'^d \simeq \Delta_3^d$ because $\boldsymbol{k}_3' \simeq \boldsymbol{k}_3$.

As is well known, a strong coupling field beam 2 will create dressed states which can be probed by scanning Δ_1 if the system is homogeneously broadened.[19] By contrast, in a Doppler broadened system since the AT splitting is usually much smaller than the Doppler width, there will be some atoms within the atomic velocity distribution which are in resonance with the dressed states. Let us consider the case when beam 2 propagates along the forward direction. According to Eq. (12), the resonant condition for $\rho_{10}^{(5)}(\boldsymbol{r},\boldsymbol{v})$ for the forward direction case is $\Delta_1^d(\Delta_1^d + \Delta_2^d) = |G_2|^2$, from which atoms with velocities $v = \pm|G_2|/k_1\sqrt{1-\zeta_2}$ will be in resonance with the dressed states in the case of $\Delta_1 = \Delta_2 = 0$ if $\zeta_2 < 1$. For these groups of atoms the resonant conditions for a three-photon transition are $\Delta_3 = \pm(1-\zeta_2+\zeta_3)|G_2|/\sqrt{1-\zeta_2}$. Thus, the SWM spectrum will exhibit a doublet structure when Δ_3 is scanned. However, due to the polarisation interference the SWM spectrum is very broad when $\zeta_2 < 1$, thus the doublet structure will be obscured. For example, Fig. 6(a) presents the SWM signal intensity versus Δ_3 with $\zeta_2 = \zeta_3 = 0.8$, $\Delta_1/\Gamma_{30} = \Delta_2/\Gamma_{30} = 0$, and $G_2/\Gamma_{30} = 0.1$ (solid curve), 30 (dashed curve) and 50 (dotted curve), showing the broadband lineshape of the SWM spectra. On the other hand, if we neglect the polarisation interference by calculating $\int_{-\infty}^{\infty}\mathrm{d}v\ \mathrm{e}^{-(v/u)^2}|\rho_{10}(\boldsymbol{r},\boldsymbol{v})|^2$, then the doublet structure of the SWM spectrum reappears, as demonstrated in Fig. 6(b) with $\zeta_2 = \zeta_3 = 0.8$, $\Delta_1/\Gamma_{30} = \Delta_2/\Gamma_{30} = 0$, and $G_2/\Gamma_{30} = 0.1$ (solid curve), 2 (dashed curve), 5 (dotted curve), and 8 (dash-dotted curve).

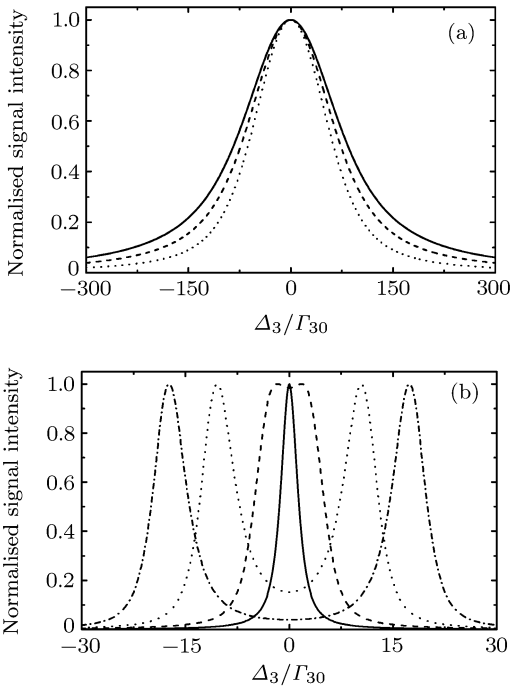


Fig. 6. SWM intensity versus Δ_3 when beam 2 propagates along the forward direction with $\zeta_2 = \zeta_3 = 0.8$, $\Delta_1/\Gamma_{30} = \Delta_2/\Gamma_{30} = 0$ and (a) $G_2/\Gamma_{30} = 0.1$ (solid curve), 30 (dashed curve), 50 (dotted curve); (b) $G_2/\Gamma_{30} = 0.1$ (solid curve), 2 (dashed curve), 5 (dotted curve), 8 (dash-dotted curve). The polarisation interference is neglected in (b).

These indicate that although the SWM spectrum is very broad due to the polarisation interference, only atoms which are in resonance with the dressed states contribute to the SWM signal.

Now, we discuss how the strong coupling field affects the SWM spectrum when the polarisation interference is significant. As shown in Fig. 6(a), counter to intuition, we see that the linewidth of the SWM spectrum becomes narrower as G_2/Γ_{30} increases. The role of the coupling field in SWM can be clarified by examining the velocity dependence of the phase of the polarisation. Let us express the off-diagonal density matrix element as $\rho_{10}^{(5)} = |\rho_{10}^{(5)}|\mathrm{e}^{\mathrm{i}\,\phi}$.

Figure 7 presents the velocity dependence of ϕ with $\Delta_1/\Gamma_{30} = \Delta_2/\Gamma_{30} = \Delta_3/\Gamma_{30} = 0$, $\zeta_2 = \zeta_3 = 0.8$, and $G_2/\Gamma_{30} = 0.1$ (solid curve), 30 (dashed curve) and 50 (dotted curve). We see that the strong field of beam 2 opens a window around $v = 0$ which increases with the increase of the coupling coefficient G_2/Γ_{30}. Within this window ϕ becomes less sensitive to the variation of the velocity, and as a result the polarisation interference becomes less destructive also. This explains why the linewidth of the SWM spectrum becomes narrower as G_2/Γ_{30} increases. A similar behaviour also occurs when beam 2 propagates along the backward direction. Finally, we investigate how the coupling coefficient G_2 affects the SWM spectrum when the spectrum is Doppler-free. Figure 8 presents the SWM spectra for forward propagation of beam 2 when Δ_3 is scanned with $\Delta_1/\Gamma_{30} = \Delta_2/\Gamma_{30} = 0$, $\zeta_2 = 1.2$, $\zeta_3 = 0.8$ and $G_2/\Gamma_{30} = 0.1$ (solid curve), 2 (dashed curve), 5 (dotted curve), and 8 (dash-dotted curve). In contrast to the previous case where the polarisation interference is significant, the SWM spectrum simply exhibits a power broadening, i.e., the linewidth increases with the increase of G_2/Γ_{30}.

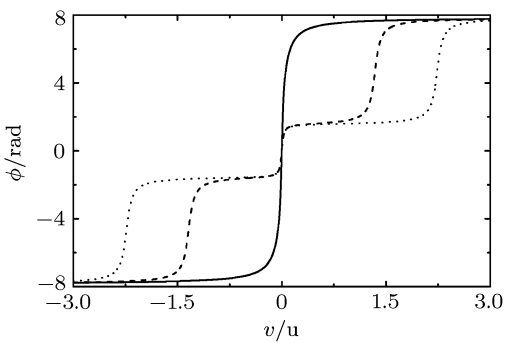


Fig. 7. Velocity dependence of ϕ when beam 2 propagates along the forward direction with $\Delta_1/\Gamma_{30} = \Delta_2/\Gamma_{30} = \Delta_3/\Gamma_{30} = 0$, $\zeta_2 = \zeta_3 = 0.8$, and $G_2/\Gamma_{30} = 0.1$ (solid curve), 30 (dashed curve), 50 (dotted curve).

This is not surprising because no atom will be in resonance with the dressed states when $\zeta_2 > 1$. Consequently, only atoms with velocity $\boldsymbol{v} \simeq 0$ will contribute to the SWM signal, thus, our system behaves more like a homogeneously broadened system.

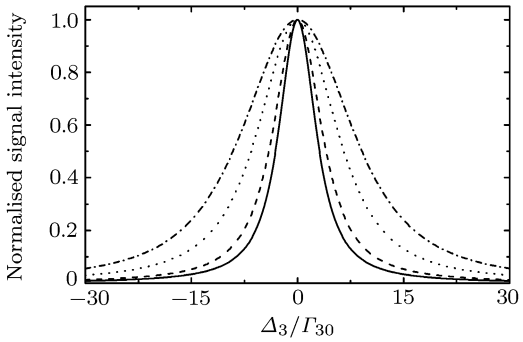


Fig. 8. SWM intensity versus Δ_3 when beam 2 propagates along the forward direction with $\Delta_1/\Gamma_{30} = \Delta_2/\Gamma_{30} = 0$, $\zeta_2 = 1.2$, $\zeta_3 = 0.8$ and $G_2/\Gamma_{30} = 0.1$ (solid curve), 2 (dashed curve), 5 (dotted curve), 8 (dash-dotted curve).

5. Conclusion

Six-wave mixing in a Doppler-broadened folded four-level system have been studied. Similar to the SWM in Doppler-broadened cascade or N-type four-level systems,[18,19] in a folded four-level system the SWM spectrum depends on whether the interference between the polarisations of atoms with different velocities is constructive or destructive. For the former case the SWM spectrum is Doppler-free, while for the latter case the spectrum becomes very broad. This polarisation interference depends on the directions of the incident beams and the ratios between the magnitudes of the wave vectors. It is found that to obtain Doppler-free SWM spectra in the folded four-level system the conditions are more stringent in comparison with those in the cascade and N-type four-level systems. Specifically, the SWM spectrum is Doppler-free only when beam 2 propagates along the direction of beam 3 and $\zeta_2 > 1$. We have also studied EIT-based SWM. For N-type or cascade four-level systems, in the presence of a strong coupling field the SWM spectrum against Δ_3 exhibits a doublet structure if the spectrum is Doppler-free.[18,19] By contrast, in the folded four-level system the strong field simply causes power broadening of the spectrum. We also find that, when the SWM spectrum is very broad, the presence of a strong coupling field can make the polarisation interference less destructive, as a result of which the SWM spectrum becomes narrower.

References

[1] Shen Y R 1984 *The Principles of Nonlinear Optics* (New York: John Wiley & Sons, Inc.)

[2] Fu P M, Jiang Q, Mi X and Yu Z H 2002 *Phys. Rev. Lett.* **88** 113902

[3] Fu P M, Mi X, Yu Z H, Jiang Q, Zhang Y P and Li X F 1995 *Phys. Rev. A* **52** 4867

[4] Mi X, Yu Z H, Jiang Q and Fu P M 1993 *Phys. Rev.* A **48** 3203

[5] Yu Z H, Mi X, Jiang Q, Li X F and Fu P M 1997 *Phys. Rev.* A **55** 2334

[6] Liu X, Niu J Y, Sun J, Mi X, Jiang Q, Wu L A and Fu P M 2008 *Acta Phys. Sin.* **57** 4991 (in Chinese)

[7] Sun J, Zuo Z C, Mi X, Yu Z H, Jiang Q, Wang Y B, Wu L A and Fu P M 2004 *Phys. Rev.* A **70** 053820

[8] Sun J, Zuo Z C, Mi X, Yu Z H, Wu L A and Fu P M 2005 *Acta Phys. Sin.* **54** 0149 (in Chinese)

[9] Moore M A, Garrett W R and Payne M G 1989 *Phys. Rev.* A **39** 3692

[10] Kang H, Hernandez G and Zhu Y F 2004 *Phys. Rev. Lett.* **93** 073601

[11] Garrett W R, Henderson S D and Payne M G 1987 *Phys. Rev.* A **35** 5032

[12] Gibson G, Luk T S, McPherson A and Rhodes C K 1991 *Phys. Rev.* A **43** 371

[13] Trebino R and Rahn L A 1987 *Opt. Lett.* **12** 912

[14] Tominaga K and Yoshihara K 1996 *Phys. Rev. Lett.* **76** 987

[15] Bolton S R, Neukirch U, Sham L J, Chemla D S and Axt V M 2000 *Phys. Rev. Lett.* **85** 2002

[16] Steffen T and Duppen K 1996 *Phys. Rev. Lett.* **76** 1224

[17] Zhang Y P, Brown A W and Xiao M 2007 *Phys. Rev. Lett.* **99** 123603

[18] Zuo Z C, Sun J, Liu X, Jiang Q, Fu G S, Wu L A and Fu P M 2006 *Phys. Rev. Lett.* **97** 193904

[19] Zuo Z C, Sun J, Liu X, Wu L A and Fu P M 2007 *Phys. Rev.* A **75** 023805

[20] Niu J Y, Wang R Q, Wang B B, Wu L A and Fu P M 2009 *J. Phys.* B: *At. Mol. Opt. Phys.* **42** 175505

[21] Niu J Y, Wang R Q, Wu L A and Fu P M 2009 *J. Opt. Soc. Am.* B **26** 2268